cis/*trans* Photoisomerization of Secondary Thiopeptide Bonds

Jianzhang Zhao,*[a, b] Jean-Claude Micheau,*[c] Carolyn Vargas,[a] and Cordelia Schiene-Fischer*[a]

Abstract: The reversible *cis*/*trans* photoisomerization of secondary thiopeptide bonds has been systematically studied with UV-visible absorption, capillary electrophoresis, ^{1}H NMR spectroscopy, and circular dichroism methods. It was found that the concentration of the *cis* conformers could be increased from less than 1% in the thermal equilibrated solution to up to 20% in the photostationary state. The rotational barriers of the thiopeptide bond and the pH dependence of the isomerization rates were also studied. The quantum yields of the *trans*→*cis* and the *cis*→*trans* processes were determined from photokinetic analysis.

Keywords: isomerization · photochemistry · photoswitching · rotational barrier · thiopeptide bonds

Introduction

As the recognition, reactivity, and stability of peptides and proteins are conformer specific, modulation of the backbone conformation of peptides or proteins has attracted great attention.[1–4] Photoswitching of the conformation of peptides is an ideal method for achieving this goal because the only external stimulus needed is light irradiation. However, the reported molecular models for photoswitching of the peptide conformation usually involve a bulky organic moiety that is not an amino acid, such as a photochromic azobenzene or spiropyran group.[2,5–8] Although some promising results have been obtained, the inherent disadvantages of this approach are the limited biocompatibility of the hybrid peptide and the problem that the final effects imposed on the backbone by the isomerizing moiety are unpredictable, that is, it is impossible to predict which peptide bond will be set in the *cis* (or *trans*) conformation following the photoswitch because the isomerization constraint is transferred from the photoresponsive center to the peptide chain through flexible bonds. Therefore, the challenge in the photomodulation of the backbone conformation of peptides is to find a novel photoresponsive constituent that can trigger the conformational change of a peptide upon illumination, by directly setting the peptide bond at a specific site in the *cis* or *trans* conformation, but that at the same time introduces only minimum perturbation of the peptide chain so that the modified peptide behaves like the native one. Unfortunately, most reported photochromic organic moieties fail to meet this critical requirement.[7] In our present study, however, the secondary thiopeptide bond has turned out to be a novel and attractive photoresponsive constituent.

Recently, the thiopeptide bond has attracted considerable interest because of its effects of conformation restriction, enhanced proteolytic stability, and modulable activity and selectivity.[9] It has been shown that the thioxylated *N*-alkylamide peptide bond is photoswitchable and that the *cis* conformer can be generated by irradiation.[10] However, for this kind of thioxylated prolyl peptide bond, the increase in *cis* conformers can also be achieved by a slow thermal equilibration process,[1] which does not take place for secondary peptide bonds. For the latter, a synthetically demanding conformation-restriction method has to be used to obtain the thermodynamically unfavorable *cis* conformers.[11,12] Here we prove that significant photoswitching occurs with secondary thiopeptide bonds and, more importantly, that the secondary thiopeptide bond can undergo dual-directional photoswitching, that is, it can be photoswitched from the *trans* conformation to the *cis* conformation and vice versa; this is different to the situation with the reported *N*-alkyl thiopeptide bonds.

A few established methods are available to study the *cis*/*trans* isomerization of peptide bonds, such as ^{1}H NMR spec-

[a] Dr. J. Zhao, C. Vargas, Dr. C. Schiene-Fischer
Max Planck Research Unit for Enzymology of Protein Folding
Weinbergweg 22, 06120 Halle/Saale (Germany)
E-mail: j.zhao@bath.ac.uk
schiene@enzyme-halle.mpg.de

[b] Dr. J. Zhao
Current address: Department of Chemistry
University of Bath, Bath BA2 7AY (UK)
Fax: (+44) 1225-826-231

[c] Dr. J.-C. Micheau
UMR 5623, Université P. Sabatier
31062 Toulouse (France)
E-mail: micheau@chimie.ups-tlse.fr

 DOI: 10.1002/chem.200400400

troscopy line-shape analysis or magnetization-transfer experiments,[13] UV-resonance Raman spectroscopy,[14] and solvent-jump and coupled assays for the *cis*→*trans* isomerization of prolyl peptide bonds.[15] However, these methods suffer from some limitations. For example, the signal-to-noise ratio is low for the UV-resonance Raman spectroscopy method and signal overlapping is often encountered with the NMR spectroscopy method.[16] In addition, these methods are usually based on the steady state (there is no or only a small shift of the *cis*/*trans* equilibrium) and they are indirect, instrumentally or technically demanding approaches for studying *cis*/*trans* isomerizations.

The study of the *cis*/*trans* isomerization of secondary amide bonds in dipeptides by monitoring the UV-visible absorption of the amide C=O groups after a jump in pH value has been reported.[17] This method is based on the shift of the *cis*/*trans* equilibrium by rapid pH variation and on the differential UV-visible absorptions of the *cis* and *trans* isomers of the secondary oxo peptide bonds. Inspired by these recent developments, we found that the *cis*/*trans* isomerization of four representative thiopeptides, H-Phe-ψ[CSNH]-Ala-OH (**1**), H-Ala-ψ[CSNH]-Phe-OH (**2**), H-Ala-ψ[CSNH]-Ala-OH (**3**), and Ac-Ala-ψ[CSNH]-Ala-NH_2 (**4**) (Scheme 1), can be studied with the UV-visible monitoring

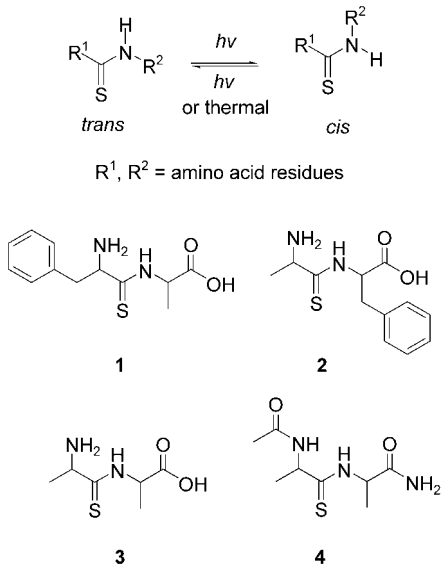

Scheme 1. Schematic representation of the *cis*/*trans* equilibrium and the structures of the *trans* conformers of the thiopeptides used in the study.

method under continuous monochromatic irradiation. Other highly sensitive methods, such as capillary electrophoresis, ^{1}H NMR spectroscopy, and circular dichroism[18] were also successfully used to characterize the *cis*/*trans* isomerizations. The rotational barrier of the thiopeptide bond was determined from temperature-variable kinetic measurements.

As the *cis*/*trans* isomerizations of secondary peptide bonds could also be crucial for the stability, recognition, and catalytic capability of proteins,[19] our studies pave the way for future conformation–activity correlation investigations of bioactive secondary peptide bonds.

Results and Discussion

UV-visible absorption: For the *N*-methyl thioacetamide or β-thiopeptides,[20–22] the UV-visible absorption, circular dichroism, and Raman spectra are different for the *cis* and *trans* conformers.[9s] Similarly, the UV-visible absorption spectrum of peptide **1** shows a significant change under UV irradiation of 254 nm, with an isosbestic point at 274 nm (Figure 1). Analogous spectral changes could also be achieved with laser irradiation at 337 nm (in this case, it is an n→π* excitation; inset of Figure 1). It is unprecedented for such a significant spectral difference to be caused by irradiation in *cis*/*trans* conformers of pseudopeptide bonds. The UV-visible spectrum of the re-equilibrated peptide solution can be fully restored and remained unchanged after several cycles of irradiation–re-equilibration. This observation indicates that the photoisomerization is fully reversible and there is no noticeable photochemical degradation during several photoisomerization cycles. Similar spectral changes are also observed for peptides **2**–**4**. On the contrary, significant photodecomposition has been observed for *N*-methyl thioacetamide and the oxo secondary peptide bonds.[14,21]

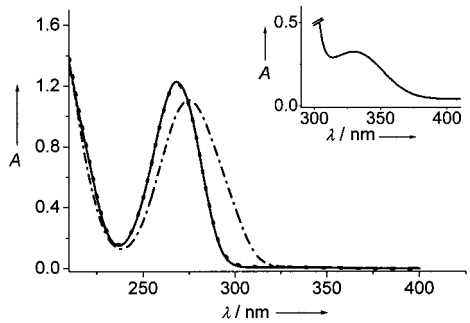

Figure 1. UV-visible absorption spectra of peptide **1** ($c = 1.4 \times 10^{-4}$ mol dm^{-3} in 5.0×10^{-2} mol dm^{-3} sodium phosphate buffer, pH 7.0, 16 °C): Equilibrated peptide (——), peptide after 3 min of irradiation at 254 nm (–•–•), and thermally re-equilibrated peptide after 4 cycles of irradiation (•••••). Inset: The $n \rightarrow \pi^*$ absorption of the equilibrated peptide at the same pH value and temperature ($c = 1.3 \times 10^{-2}$ mol dm^{-3}).

Figure 1 shows that the *cis* conformer of peptide **1** has a stronger absorption near 300 nm, whereas the *trans* conformer gives a stronger absorption near 270 nm. Therefore, the equilibrium of the *cis* and *trans* conformers of **1** is dual-directionally photoswitchable.[23] Similar results were also observed for **2**–**4**.

Capillary electropheresis (CE): The irradiated solutions of peptides **1**–**4** were also investigated by high-performance CE.[23,24] When the new electropherogram was compared to the electropherogram of the nonirradiated peptide, it could be seen that a new peak appeared after irradiation. This peak was assigned to the *cis* conformer, which was generated by irradiation (supported by its UV-visible spectrum, obtained in situ with a diode-array CE instrument), and its relative concentration was determined to be about 9% for peptide **1**. By extrapolating to the photostationary state

(PSS), the *cis* concentration has been corrected as 11% at pH 3.0, 20% at pH 4.0, and 19% at pH 7.0. The new peak disappeared completely after sufficient re-equilibration time. The reversibility of the electropherogram offers another confirmation that the change in the UV-visible absorption was caused by reversible *cis*/*trans* isomerization of the secondary thiopeptide bond. The UV-visible spectra determined in situ gave a reliable absorption-peak position for the *cis* and *trans* isomers and confirmed that the isosbestic point is indeed at 275 nm. Our method offers a new approach for the direct determination of the UV-visible absorption spectrum of the unstable *cis* conformers, a tough task that usually has to be done by indirect spectra analysis.[25] However, it should be noted that this CE approach is limited to systems exhibiting sufficiently slow isomerization rates.

^{1}H NMR spectra analysis: ^{1}H NMR was also used to study the changes of peptide **1** with irradiation (Figure 2). After irradiation, a peak assigned to the *cis* conformer appeared (in

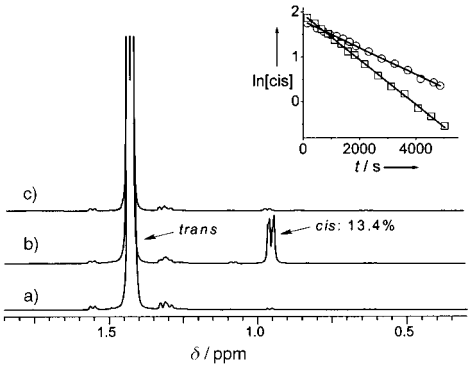

Figure 2. ^{1}H NMR spectra of peptide **1** with irradiation ($c = 3.0 \times 10^{-2}$ mol dm^{-3} in D_2O). The alanine CH_3 region at 1.4 ppm is shown. (The signal of the *cis* conformer appears at 0.9 ppm.): a) Thermally equilibrated peptide solution, b) peptide after 45 min of irradiation at 254 nm, and c) peptide after 30 min relaxation in darkess at 5°C. Inset: Evolution of the first-order re-equilibration of the irradiated peptide **1**, as monitored through the concentration of the *cis* conformer. $k_{obsd} = (2.98 \pm 0.03) \times 10^{-4}$ s^{-1} at 5°C (○) and $k_{obsd} = (5.04 \pm 0.05) \times 10^{-4}$ s^{-1} at 10°C (□).

the alanine CH_3 region)[16] and its ratio was determined to be around 13%. Under these conditions, the *cis* concentration at the PSS was determined to be about 14% (pH 7.0), a value that roughly agrees with the CE analysis. The percentage of the *cis* conformer at the PSS is affected by several factors, such as the wavelength and the power of the irradiation, the temperature, and so forth. By monitoring the thermal re-equilibration (inset of Figure 2), the first-order *cis*/*trans* isomerization rate constant (k_{obsd}) was determined to be $(2.98 \pm 0.03) \times 10^{-4}$ s^{-1} at 5°C and $(5.04 \pm 0.05) \times 10^{-4}$ s^{-1} at 10°C. These results agree with those derived from the photoswitch UV-visible absorption data, for which the k_{obsd} values are of the same order of magnitude (2.95×10^{-4} s^{-1} at 5°C and 5.29×10^{-4} s^{-1} at 10°C).

Circular dichroism (CD) analysis: As the *cis*/*trans* isomerization of the thiopeptide bonds occurs in the proximity of chiral centers, the CD spectrum should report such bond-rotation events.[10] After irradiation, the CD response of peptide **1** at 268 nm changed to the opposite sign (Figure 3a).

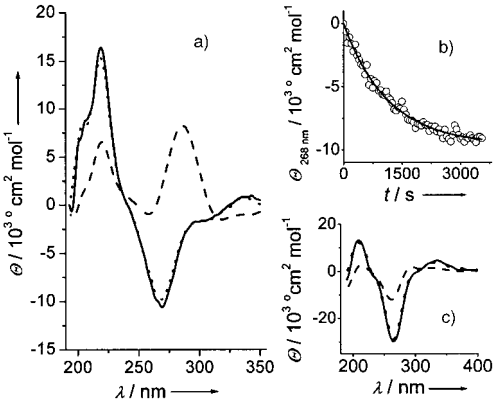

Figure 3. a) CD spectra of peptide **1** with irradiation ($c = 1.4 \times 10^{-4}$ mol dm^{-3} in a 5.0×10^{-2} mol dm^{-3} sodium phosphate buffer, pH 7.0, 14°C): Thermally equilibrated peptide (——), peptide after irradiation at 254 nm for 3 min (-----), and re-equilibrated peptide (•••••); b) first-order evolution of the 268 nm molar ellipticity of peptide **1** after irradiation at 254 nm for 1 min: $k_{obsd} = (8.73 \pm 0.14) \times 10^{-4}$ s^{-1}; c) CD spectra of peptide **3** ($c = 1.2 \times 10^{-4}$ mol dm^{-3} in 5.0×10^{-2} mol dm^{-3} sodium phosphate buffer, pH 7.0, 16°C): Thermally equilibrated peptide (——), peptide after irradiation at 254 nm for 3 min (-----), re-equilibrated peptide (•••••).

This finding suggests that the molecular geometry around the chromophore (C=S) was changed significantly upon irradiation. After re-equilibration, the original CD spectrum was fully recovered. The molar ellipticity at 268 nm was used to monitor the re-equilibration process. At 14°C, a first-order rate constant of $k_{obsd} = (8.73 \pm 0.14) \times 10^{-4}$ s^{-1} was obtained (Figure 3b), which was comparable to those obtained from UV-visible absorption spectroscopy ($k_{obsd} = (8.43 \pm 0.01) \times 10^{-4}$ s^{-1}). Peptides **2**–**4** gave similar results (as an example, the result with peptide **3** is depicted in Figure 3c).

Rotation barrier of the thiopeptide bond ($\Delta G^{\ddagger}$): As it has been established that the *cis*/*trans* isomerization was caused by photoswitching, the UV-visible absorbance at 290 nm was used to monitor the re-equilibration process of peptide **1** after irradiation.[17] The nonlinear single-exponential regression of the relaxation curve gave a first-order rate constant of $k_{obsd} = (1.04 \pm 0.00) \times 10^{-3}$ s^{-1} (16°C) and a determination coefficient of $r^2 = 0.9999$. The perfect fitting of the experimental data shows that the process is a well-defined first-order reaction, as expected for a *cis*/*trans* isomerization of peptide-bond conformers. A pH-jump experiment (inset of Figure 4), which is known to be able to shift the *cis*/*trans* equilibrium of peptide bonds with ionizable side chains,[17] gave a similar rate constant of $k_{obsd} = (9.70 \pm 0.17) \times 10^{-4}$ s^{-1} ($r^2 = 0.8805$). However, the signal-to-noise ratio for the photoswitch method is greatly improved over that of the pH-jump experiments (Figure 4 and the r^2 values). Therefore, the *cis*/*trans* isomerization rate constants of peptides **2**–**4** were also studied by using a similar photoswitch method.

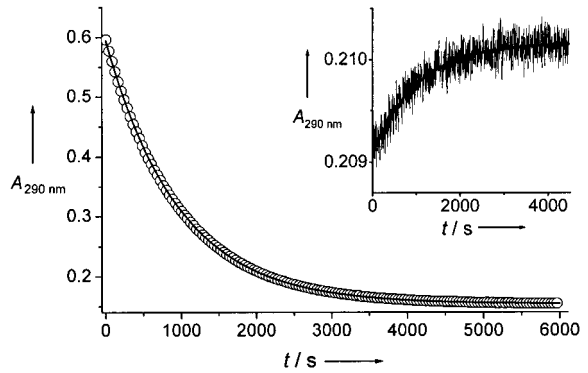

Figure 4. Time course of *cis*-to-*trans* reverse isomerization of peptide **1** (1.4×10^{-4} mol dm^{-3} in 5.0×10^{-2} mol dm^{-3} sodium phosphate buffer, pH 7.0, 16 °C) after irradiation at 254 nm for 2 min. *Cis*/*trans* isomerization rate constant $k_{obsd}=(1.04\pm0.00)\times10^{-3}$ s^{-1} ($r^2=0.9999$). Inset: Time course of *cis*/*trans* isomerization of peptide **1** following a pH jump (pH 1.1→6.9). Peptide **1** (1.2×10^{-3} mol dm^{-3}) in HCl (0.1 mol dm^{-3}; pH 1.1) was diluted 16-fold in sodium phosphate buffer (0.05 mol dm^{-3}; pH 7.0) at 16 °C. *Cis*/*trans* isomerization rate constant $k_{obsd}=(9.70\pm0.17)\times10^{-4}$ s^{-1} ($r^2=0.8805$). The solid lines represent the single-exponential nonlinear regression. For clarity, only some of the recorded data points are displayed.

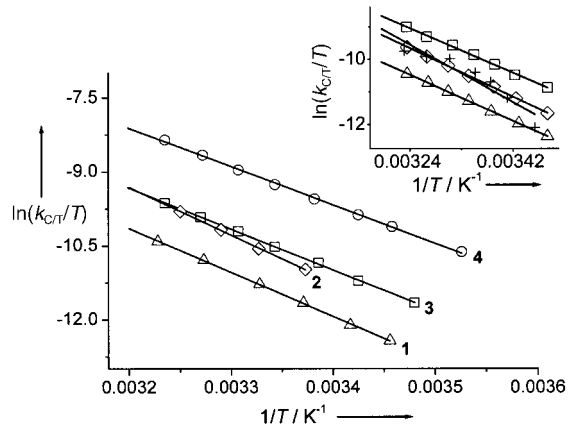

Figure 5. Eyring plots of the *cis*/*trans* isomerization of the thiopeptides **1**–**4** (6.0×10^{-4} mol dm^{-3} peptide in 5.0×10^{-2} mol dm^{-3} sodium phosphate buffer, pH 7.0): Peptide **1** (△), peptide **2** (◇), peptide **3** (□), and peptide **4** (○). Inset: Eyring plot of peptide **3** at pH 3 (□), pH 5 (◇), and pH 9 (△). The result obtained from the solvent-mediated pH-jump (from 1.7 to 6.9) is also included (+). Error bars (1–2 %) for the respective k_{obsd} values at different temperatures are omitted for clarity.

The temperature dependence of the isomerization rate constants k_{obsd} were analyzed by using Eyring plots to obtain the activation enthalpy and entropy of the rotation (Figure 5). The activation parameters for the rotational barrier of peptides **1**–**4** are listed in Table 1. Due to the greatly improved signal-to-noise ratio, the photoswitch method gave Eyring plots with much better linearity (shown by r^2, Table 1). The results of the activation energy are in reasonable agreement with the reported rotational barrier for the Ala–Ala peptide bond (69.9 kJ mol^{-1})[17] and the theoretical calculations that the rotational barrier of thiopeptide bond will be increased in comparison to that of oxo peptide bonds.[26] The cationic, zwitterionic, and anionic forms have different rotational barriers. This effect is caused by the different driving forces lying on the opposite charges on the N terminus and the C terminus of the peptides.[13] The rotational barrier is sensitive to the amino acid sequence of the thiopeptides. To the best of our knowledge, this is the first successful measurement of the rotational barrier of thiopeptide bonds, based on a facile, yet accurate, spectroscopic method.

pH Dependence of the *cis*/*trans* isomerization rate constants (k_{obsd}): The pH dependence of the *cis*/*trans* isomerization rate constants k_{obsd} of thiopeptides **1**–**3** was also studied in detail (Figure 6).[27] The results were applied to the modified Henderson–Hasselbalch equation.[17] The k_{obsd}/pH profile of peptide **1** is drastically different from that of the oxo dipeptides (for example, the profile of the oxo peptide Ala–Ala, shown as a dotted line in Figure 6). The slower *cis*/*trans* isomerization will result in an increased rotation barrier ($\Delta G^{\neq}$). For all pH-sensitive peptides such as **1**–**3**, the rotational barrier is higher in the anionic form than in the cationic form (Table 1). The k_{obsd}/pH profile of peptides **2** and

Table 1. Characteristic kinetic and thermodynamic parameters for the *cis*/*trans* isomerization of the thiopeptide bond of compounds **1**–**4**.

	k_{obsd}[a] [s^{-1}]	k_{obsd}[b] [s^{-1}]	$\Delta H^{\neq}$[c] [kJ mol^{-1}]	$\Delta S^{\neq}$[c] [J mol^{-1} K^{-1}]	$\Delta G^{\neq}$[d] [kJ mol^{-1}]	r^2[e]
1+	$(1.60\pm0.00)\times10^{-2}$	$(1.25\pm0.07)\times10^{-2}$	67.9±1.5	−53.7±5.0	84.0	0.9975
1±	$(3.79\pm0.00)\times10^{-3}$	$(3.24\pm0.34)\times10^{-3}$	74.4±0.7	−44.0±2.3	87.6	0.9996
1−	$(1.82\pm0.00)\times10^{-3}$	$(1.55\pm0.32)\times10^{-3}$	80.1±1.0	−32.0±3.7	89.7	0.9993
2+	$(2.39\pm0.01)\times10^{-2}$	$(1.66\pm0.10)\times10^{-2}$	66.7±1.2	−54.3±4.0	83.0	0.9994
2±	$(8.04\pm0.02)\times10^{-3}$	$(8.21\pm0.40)\times10^{-3}$	80.3±1.4	−18.3±4.7	85.8	0.9994
2−	$(2.85\pm0.01)\times10^{-3}$	$(3.02\pm0.42)\times10^{-3}$	83.6±1.3	−16.0±4.3	88.4	0.9995
3+	$(3.72\pm0.01)\times10^{-2}$	$(2.79\pm0.24)\times10^{-2}$	67.5±0.8	−47.3±2.7	81.7	0.9972
3±	$(9.32\pm0.01)\times10^{-3}$	$(8.68\pm0.94)\times10^{-3}$	68.9±0.7	−54.7±2.3	85.3	0.9995
3±[f]	$(8.45\pm0.03)\times10^{-3}$	–	81.6±12.7	−12.7±42.3	85.4	0.8923
3−	$(5.84\pm0.01)\times10^{-3}$	$(3.17\pm1.37)\times10^{-3}$	65.3±0.4	−73.3±3.3	87.3	0.9998
4	$(3.17\pm0.01)\times10^{-2}$	–	64.7±0.9	−58.0±3.0	82.1	0.9989

[a] k_{obsd} value of the cationic (+), zwitterionic (±), or anionic (−) forms of the peptides at pH 2.0, 7.0, and 9.0, respectively, and at 27 °C. [b] k_{obsd} value from the fitting of the k_{obsd}/pH value profile obtained with the modified Henderson–Hasselbalch equation for measurements taken at 27 °C. [c] $\Delta H^{\neq}$ and $\Delta S^{\neq}$ values from the Eyring plots at pH 2.0, 7.0, and 9.0, for the cationic (+), zwitterionic (±), and anionic (−) forms of the peptides, respectively. $\Delta H^{\neq}$ and $\Delta S^{\neq}$ were obtained simultaneously with the Eyring plot. [d] $\Delta G^{\neq}$ value from the Gibbs equation for measurements taken at 27 °C. [e] Determination coefficients of the Erying plot fitting. [f] The data were obtained from pH-jump experiments.

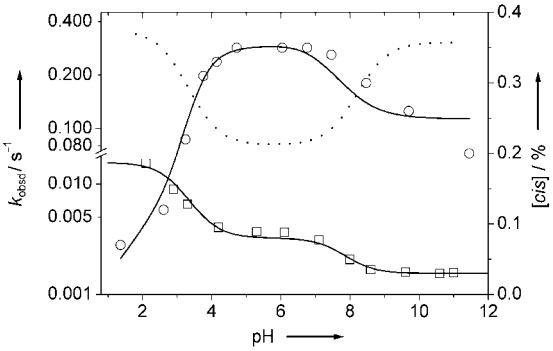

Figure 6. pH dependence of the *cis*/*trans* isomerization rate constants (k_{obsd}) for peptide **1** after photoswitching ($c = 6.0 \times 10^{-4}$ mol dm^{-3} in a 0.05 M phosphate buffer at various pH values, 27 °C; marked by □, left vertical axis scale). The pH-dependence profile of the k_{obsd} for the peptide Ala–Ala is included as a comparison (·····, left vertical axis scale).[17] pH dependence of the *cis* content of peptide **1** (marked by ○, right vertical axis scale; determined by the ^{1}H NMR spectroscopy method at 27 °C). The solid lines represent the calculated curves according to the modified Henderson–Hasselbalch equations with pK_a values of 3.0 (COOH) and 7.7 (NH_3^+). Error bars (1–2 %) for the respective k_{obsd} values are omitted for clarity.

3 shows a similar result. For the thiopeptides, the k_{obsd} value at high pH values is much smaller than that in low pH conditions. It is preliminarily supposed that the thermodynamically unfavorable *cis* conformers of thiopeptides **1**–**3** are kinetically stabilized at high pH values, possibly by an intramolecular hydrogen bond (COO^- at the C terminal as a hydrogen-bond acceptor and CS–NH as a hydrogen-bond donor).[22] The ^{1}H NMR spectroscopy temperature coefficient of the thioamide proton of peptide **1** was determined to be around -4.45 ppb K^{-1}. Such a value supports our hypothesis because it is known that if the temperature coefficient of the amide proton is higher than -4.5 ppb K^{-1} then it is highly possible that an intramolecular hydrogen bond exists.[28]

Based on the equilibrium constant for peptide **1** (NMR spectroscopy determination), and the Henderson–Hasselbach simulation, the respective isomerization rate constants of the *cis*→*trans* ($k_{C\to T}$) and *trans*→*cis* ($k_{T\to C}$) processes were derived (Table 2). The results show that the rate constant for the spontaneous process of *trans*→*cis* can be neglected and the variation of the k_{obsd} values at different pH values (Figure 6) was mainly due to the change in the rate constant of the *cis*→*trans* process ($k_{C\to T}$).

From the *cis* content/pH profile, the free Gibbs energy gap for the *cis* and *trans* isomer of peptide **1** ($\Delta G°$) was found to vary from 14.1 kJ mol^{-1} in the zwitterionic form to 19.2 kJ mol^{-1} in the cationic form. This result confirms that the free Gibbs energy gap of the *cis* and *trans* peptide-bond conformers, which is usually smaller than 8.4 kJ mol^{-1} in oxo peptides, has been increased by thioxylation.[26,29]

Determination of the photoisomerization quantum yields: For photokinetic analysis purposes,[30–38] the above *cis*/*trans* photoisomerizable thiopeptides can be considered as the well-known (2Φ, $1k$) model.[34] The whole process involves two photoisomerizations (*trans*→*cis* and *cis*→*trans*; hence there are two unknown quantum yields or 2Φ) and one thermal relaxation (*cis*→*trans*; hence there is one first-order rate constant or $1k$, which can be determined from relaxation monitoring). The thermal process from *trans* to *cis* was neglected.

The two quantum yields were determined with sufficient accuracy from the photokinetic analysis of absorbance versus time curves recorded under continuous monochromatic irradiations. The analysis compares the effect of the irradiation, which promotes the *trans* to *cis* isomerization, to the effect of the thermal relaxation of the *cis* to the *trans* isomerization. However, as the effect of the irradiation is not only the *trans* to *cis* photoisomerization, but also the reverse process, it was necessary to use at least two different irradiation wavelengths in order to vary the relative importance of the two photochemical processes. This approach, which does not need previous knowledge of the spectrum of the unstable conformer, is particularly useful when the photoisomer is too labile to be easily isolated. From the practical point of view, the rates of the three processes are used to establish a differential equation [Table 3; Eq. (1)] that gives rise to the evolution of the concentration of the *trans* (T) species (see the Experimental Section for more details).

Table 3. Primary photo- and thermal reactions used for the photokinetic analysis (I_0 is the photon flux and F is the photokinetic factor).

Process	Rate
trans (T)→*cis* (C) (Φ_{TC})	$v_1 = \Phi_{TC}\varepsilon'_T[T]lI_0F$
cis (C)→*trans* (T) (Φ_{CT})	$v_2 = \Phi_{CT}\varepsilon'_C[C]lI_0F$
cis (C)→*trans* (T) (k_Δ)	$v_3 = k_\Delta[C]$

$$d[T]/dt = -v1 + v2 + v3 \quad (1)$$

at PSS, $d[T]/dt = 0$, and $v1 = v2 + v3$

Table 2. *Cis*/*trans* isomerization rate constants ($k_{C\to T}$ and $k_{T\to C}$) for the secondary thiopeptide bond in peptide **1** in the cationic (**1**+), zwitterionic (**1**±), and anionic (**1**−) forms.

	1+	**1**±	**1**−
cis conformer [%][a]	0.045	0.35	0.275
k_{obsd} [s^{-1}][b]	$(1.25 \pm 0.07) \times 10^{-2}$	$(3.24 \pm 0.34) \times 10^{-3}$	$(1.55 \pm 0.32) \times 10^{-3}$
$k_{C\to T}$ [s^{-1}][c]	$(1.25 \pm 0.07) \times 10^{-2}$	$(3.23 \pm 0.34) \times 10^{-3}$	$(1.55 \pm 0.32) \times 10^{-3}$
$k_{T\to C}$ [s^{-1}][c]	$(5.65 \pm 0.32) \times 10^{-6}$	$(1.14 \pm 0.12) \times 10^{-5}$	$(4.28 \pm 0.88) \times 10^{-6}$

[a] Determined by ^{1}H NMR analysis and the modified Henderson–Hasselbalch equation (see Figure 6). [b] From the fitting of the k_{obsd}/pH value profile with the modified Henderson–Hasselbalch equation. [c] According to the equilibrium constants and the equations $k_{obsd} = k_{C\to T} + k_{T\to C}$ and $k_{C\to T} = k_{obsd}(1 - \%\ cis)$. The error limits for $k_{C\to T}$ and $k_{T\to C}$ were estimated from that of k_{obsd}.

Beer's law and mass balance are used for the calculation of the absorbance at any wavelength [Eq. (2)], where $[T_0]$ is the initial concentration of the thiopeptide in its stable *trans* form, ε_T and ε_C are the absorbtion coefficients of the *trans* and *cis* isomers, respectively, and l is the pathlength.

$$\text{Absorbance} = [(\varepsilon_T - \varepsilon_C)[T] + \varepsilon_T[T_0]]l \quad (2)$$

The variations of the absorbance at the two irradiation and three monitoring wavelengths were recorded (Figure 7). The quantum yields and several absorption coefficients were optimized simultaneously to achieve numerical fitting. The results for peptides **2**–**4** are gathered in Table 4. (We failed to obtain accurate quantum yields for compound **1**.)

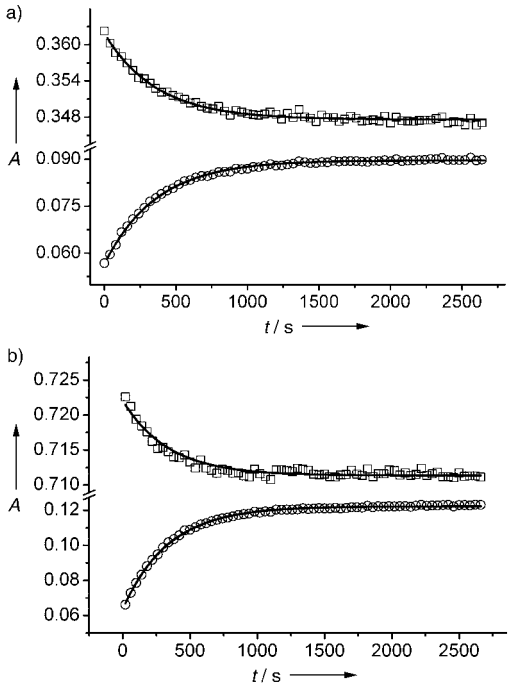

Figure 7. Evolution of the absorbance of peptide **3** (6.0×10^{-5} mol dm^{-3} in 0.05 M sodium phosphate buffer, pH 7.0, 16 °C) with continuous irradiation. Top: Irradiation at 252 nm, 16 °C: □ = absorbance at 252 nm; ○ = absorbance at 290 nm. Bottom: Irradiation at 266 nm: □ = absorbance at 266 nm; ○ = absorbance at 290 nm. The four experimental curves were fitted simultaneously from Equations (1) and (2) by using parameter values from Table 4 (solid lines represent the fitting result). For clarity, only half of the recorded raw data points are displayed.

The photoisomerization quantum yields are comparable to those of oxo peptide bonds, lying in the range of 0.075–0.12 as determined by Raman spectroscopy.[35] For the nonaromatic peptides **3** and **4**, the reverse quantum yield (Φ_{CT}) remains low. From the calculations, the spectra of the *cis* conformers can be reconstructed. Figure 8 allows a comparison between the UV-visible spectra of the *trans* and *cis* conformers for thiopeptide **3**, as determined from CE and reconstructed from photokinetic analysis. The good agreement between the two results indicates the validity of our photokinetic quantum yield determinations. The calculated *cis* concentration at PSS (Table 4) is different from the CE and NMR spectroscopy results. However, this difference is easily understandable by taking into account the different experimental conditions.

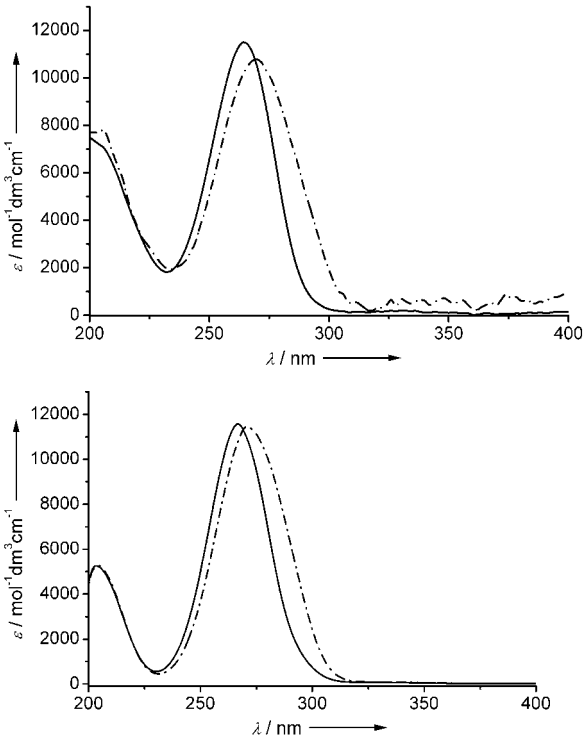

Figure 8. The UV-visible absorbance spectra of the *trans* (——) and the *cis* (–•–•) conformers of peptide **3**. Top: Spectra determined in situ by CE. Bottom: Spectrum of *trans* form determined by UV-visible spectrometry and spectrum of *cis* form determined from photokinetic analysis.

Table 4. Photokinetic parameters of the *cis*/*trans* photoisomerization of thiopeptides **2**–**4**, back-isomerization rate constants ($k_{C\to T}$, experimental determination), photon flux (experimental determination), quantum yield of the *trans*-to-*cis* process ($\Phi_{T\to C}$) and the *cis*-to-*trans* process ($\Phi_{C\to T}$), *cis* concentration at the PSS (numerical determination, *cis*/*trans* ratio at the PSS is given by $[C]/[T]_{PSS} = \Phi_{TC}\varepsilon'_T I_0 F/(\Phi_{CT}\varepsilon'_C I_0 F + k_{C\to T})$), and extinction coefficients of the *trans* and *cis* conformers (numerical determination). Peptide solution in 5.0×10^{-2} mol dm^{-3} sodium phosphate buffer (pH 7.0, 16 °C).

		2	**3**	**4**
$k_{C\to T}$ [s^{-1}]		$(2.07\pm0.00)\times10^{-3}$	$(2.64\pm0.00)\times10^{-3}$	$(1.06\pm0.00)\times10^{-2}$
photon flux (I_0) [mol^{-1} dm^3 cm^{-1}]	252 nm	1.11×10^{-7}	8.52×10^{-8}	8.24×10^{-8}
	266 nm	1.36×10^{-7}	1.27×10^{-7}	1.29×10^{-7}
quantum yields (Φ)	$\Phi_{T\to C}$	0.13	0.16	0.18
	$\Phi_{C\to T}$	0.60	0.04	0.01
[*cis*] at the PSS [%]	252 nm	4.0	5.0	1.0
	266 nm	7.0	8.5	3.0
ε_{trans} (ε_{cis}) [mol^{-1} dm^3 cm^{-1}]	252 nm	3900 (600)	6000 (4100)	6400 (1400)
	266 nm	8200 (4500)	11600 (10300)	10800 (7000)
	290 nm	1200 (10700)	2500 (7300)	600 (9700)

The photoswitch effect discussed above was also applicable to oligothiopeptides, such as the His[12]-thio-S-peptide (a peptide with 20 amino acid residues).[23] Preliminary results show that the activity of the

modified ribonuclease, obtained with the above S-peptide and S-protein, can be modulated by photoswitching.

Conclusion

In summary, a significant *cis*/*trans* photoisomerization ability was found for secondary thiopeptide bonds and was used to characterize the *cis*/*trans* isomerization of four representative thiopeptides. Due to the spectral differences between the *cis* and *trans* conformers, the *cis*/*trans* photoisomerization was systematically studied with UV-visible absorbance, capillary electrophoresis, circular dichroism, and NMR spectroscopy methods. The quantum yields of the *cis*/*trans* photoisomerization were determined by using photokinetic analysis. From temperature-variation kinetic measurements, it was shown that the thioxylated peptide bond has higher rotation barriers than the normal oxo peptide bond. Thus, the thiopeptide bonds shows much slower thermal re-equilibration rates than the normal oxo peptide bonds; this is important for the photomodulation of the peptide backbone conformation and the bioactivity. Moreover, in comparison to the results with the normal peptides, the *cis*/*trans* isomerization of the thiopeptide bonds is retarded at high pH values. With the photoswitch method, this work offers the first opportunity of a panoramic insight into the *cis*/*trans* isomerization of thiopeptide bonds. With secondary thiopeptide bonds as the photoresponsive constituent, the photoisomerization capability can be directly coupled to the peptide backbone in an efficient and precise way. Further studies will concentrate on the photoregulation of the conformation and consequently of the bioactivity of peptides or proteins.

Experimental Section

General: Peptides **1**–**4** were synthesized according to the reported methods.[9l,39] The products were lyophilized and analyzed with HPLC, MS (ESI), and ^{1}H and ^{13}C NMR spectroscopy. A standard laboratory UV lamp was used in the irradiation, with a wavelength of 254 nm and an intensity of 2 mW cm^{-2}. The wavelength-tunable monochromatic light source was described previously.[23] Data analysis of the time-course curves, performed by single-exponential nonlinear regression by using a SigmaPlot scientific graphing system (Version 2000), gave the isomerization rate constants (k_{obsd}).

UV/Vis absorption spectra: The UV/Vis difference spectra for the peptide-bond isomers of peptides **1**–**4** were evaluated from the spectra of the peptides before and after 254 nm irradiation. A Hewlett–Packard 8452A diode-array UV/Vis spectrophotometer was used for monitoring the UV/Vis spectra during continuous irradiation. The integration time for the acquirement of the spectra was set as the minimal value of 0.1 s to minimize the side effects of the probe beam of the diode-array instrument.

^{1}H NMR spectroscopy: All NMR measurements were performed on a Bruker ARX 500 spectrometer operating at a 500.13 MHz proton frequency. The *cis* content/pH value study of the peptides was performed at 27 °C with a peptide concentration of 2×10^{-2} mol dm^{-3} in solution. The final pH value was adjusted with HCl and NaOH. The ^{1}H NMR spectra of the irradiated peptide was recorded at 5 °C and 10 °C, with a peptide concentration of 3×10^{-2} mol dm^{-3} in solution (pH 7.0). The standard (254 nm) UV lamp was used in the irradiation. The irradiated sample was transferred into the spectrometer immediately after irradiation. The typical time interval between the termination of irradiation and the start of measurement was 1.5 min. The pK_a values of the peptide side chains were determined by the pH titration method.

Capillary electrophoresis (CE): A Beckman P/ACE system MDQ capillary electrophoresis instrument was used. The analyses were carried out with the following conditions: 0.05 mol dm^{-3} sodium phosphate buffer with the desired pH value was used as the running buffer, 30×25 μm fused silica capillary, separation voltage of 25 kV, capillary temperature of 2 °C, UV detection at the isosbestic point of the *cis* and *trans* conformers of the thiopeptides. The irradiated peptide solution was transferred into the CE instrument immediately after irradiation. The typical time interval between the termination of irradiation and the start of measurement was 2 min. The typical migration time was about 210–270 s. The *cis*/*trans* ratios were determined by Gaussian fitting of the CE peaks.

Circular dichroism (CD): The CD spectra of the peptides were recorded with a J-710 spectropolarimeter and a 1 mm CD cuvette. For the determination of the CD spectrum without irradiation, 10 accumulations were used. For the determination of the CD spectra of the irradiated peptide solution, however, only 1 accumulation was used and the irradiation/recording experiment was repeated 10 times. The final spectrum was the mean result of 10 raw spectra. The temperature of the CD cuvette was controlled by circulating water from a thermostat (±0.1 °C; Haake D8, Germany).

Determination of the rotational activation energies and the k_{obsd}/pH value profile: The peptide solution (1.4×10^{-4} mol dm^{-3} in 0.05 mol dm^{-3} sodium phosphate buffer) was thermally equilibrated for 5 min before each experiment by putting the sample in the cuvette holder, then irradiated with the laser or UV lamp at the desired pH value and temperature. After irradiation, the time course of the absorption at 290 nm was monitored with a PerkinElmer UV/Vis/NIR Lambda 900 spectrometer. The solution was continuously stirred with a magnetic bar within the cuvette to ensure homogeneity. The temperature of the cuvette holder was controlled by circulating water from a thermostat (±0.1 °C; Haake D8, Germany). The temperature was measured directly with a microthermoprobe within the cuvette. For the pH-jump experiments, a solution of peptide **1** (1.2×10^{-3} mol dm^{-3}) in HCl (0.1 mol dm^{-3}) at pH 1.1 was 100-fold diluted into 0.05 mol dm^{-3} sodium phosphate buffer at pH 7. The time course of the absorption at 290 nm was monitored. The final pH value was measured at the end of the monitoring process. In order to calculate the rotational barriers, the temperature dependency of the isomerization rate constants was studied and the data were applied to the Eyring plot to obtain the activation enthalpy, $\Delta H^{\neq}$ (in J mol^{-1}), and the activation entropy, $\Delta S^{\neq}$ (in J mol^{-1} K^{-1}), values, according to Equation (3), in which k_{obsd} (in s^{-1}) is the observed first-order rate constant, T is the experimental temperature (in K), R is the universal gas constant, k_B is the Boltzmann constant, and h is the Planck constant. The rotational barriers were calculated according to the Gibbs equation [Eq. (4)].

$$\ln(k_{obsd}/T) = (-\Delta H^{\neq}/R)(1/T)+\Delta S^{\neq}/R+\ln(k_B/h) \quad (3)$$

$$\Delta G^{\neq} = \Delta H^{\neq} - T\Delta S^{\neq} \quad (4)$$

The energy gaps between the *trans* and the *cis* conformers were determined with the van't Hoff equation [Eq. (5)], in which the equilibrium constant, K, was readily calculated from the *cis*/*trans* ratio of the equilibrated solution, as determined with the NMR spectroscopy method.

$$\Delta G^{o} = -RT\ln K \quad (5)$$

For the k_{obsd}/pH value study, the *cis*/*trans* isomerization rate constants of the thiopeptides were determined at different pH values and the rate constants were applied to the modified Henderson–Hasselbalch equation [Eq. (6)]. In this equation, k_{obsd} is the isomerization rate constant determined experimentally, k_+, $k_\pm$, and k_- are the isomerization constants of the cationic, zwitterionic, and anionic forms of the thiopeptides (to be numerically fitted), respectively, pK_a^1 and pK_a^2 are the acidic and basic pK_a values of the peptides (determined with the NMR titration method), respectively, and x is the variable pH value. This equation was imbedded within the SigmaPlot scientific graphing system (Version 2000) and the numerical fitting gave the k_+, $k_\pm$, and k_- values.

$$k_{obsd} = k_{+}/\{10^{(x-pK_a^1)} \times [1+10^{(x-pK_a^2)}]\} + k_{\pm}/[1+10^{(x-pK_a^2)}] + [k_{-} \times 10^{(x-pK_a^1)} \times 10^{(x-pK_a^2)}]/\{10^{(x-pK_a^1)} \times [1+10^{(x-pK_a^2)}]\} \quad (6)$$

Photokinetic monitoring of the *cis*/*trans* photoisomerization: A Hewlett–Packard 8452A diode-array UV/Vis spectrophotometer was used for multiwavelength monitoring of the absorption changes of the peptide solution during continuous irradiation. The wavelength and resolution of the home-assembled monochromatic light source were calibrated with the diode-array UV/Vis spectrophotometer. The typical bandwidth of the monochromatic beam is less than 8 nm. The monochromatic light intensity of the continuous irradiation beam was measured with a DR-1600 digital radiometer (24600-Si diode detector with an active area of 1 cm^2; Gamma Scientific, USA). The peptide solution was continuously stirred with a hydrodynamic bar within the photoreactor to ensure homogeneity. The temperature of the photoreactor holder was controlled by circulating water from a thermostat (±0.1 °C; Haake D8, Germany). The temperature was measured directly with a microthermoprobe within the reactor. The internal volume of the reactor was 2.0 mL. The photoreactor had an optical pathlength of 1.6 cm. The data sampling time was set as 1 point per 20 seconds and the integration time (the opening of the shutter of the spectrophotometer) of each data point was 0.1 seconds. A control experiment showed that such a sampling setting does not cause any photoisomerization. A higher sampling frequency is not recommended because the probe beam of the diode array spectrophotometer causes undesired photoconversion. It should be noted that in this case a continuous scanning spectrophotometer (double beam, with a photomultiplier-tube detector) was not applicable. For each experiment, the absorbance was recorded at two wavelengths (one being the irradiation wavelength).

Determination of the quantum yields from photokinetic analysis of the absorbance (Abs) versus time curves: The (2Φ, 1k) model[34] was used, thereby giving rise to Equations (1) and (2). Four independent photokinetic curves were recorded at two irradiation wavelengths. The parameters to be determined were the quantum yields, the molar extinction coefficients of the *trans* and the *cis* isomers, and the rate constant of thermal re-equilibration. Most of them could be reached from independent measurements. The UV/Vis spectra of the *trans* and the *cis* isomers of the thiopeptide bonds could be preliminarily determined with CE analysis, based on the separation of the *cis* and the *trans* conformers. The isomerization rate constant values for $k_{C\rightarrow T}$ (k_Δ) were extracted separately from the kinetics of the reverse isomerization in the dark at the same temperature. Experimental photokinetic curves (Abs_{exp} versus t) were fitted by the model (Abs_{calcd} versus t). The calculated curves were obtained from the numerical integration of the differential kinetic equation by using a Runge–Kutta semi-implicit procedure for the concentrations and the Beer's law for the absorbencies. The photokinetic factor $F = (1-10^{-Abs'})/Abs'$ was continuously monitored with the records of the absorbance at the irradiation wavelength (Abs′). The residual error function $RE = \Sigma_p\Sigma_j(Abs_{calcd}(j) - Abs_{exp}(j))^2/pj$ (where p is the number of plots fitted simultaneously and j is the number of points in each plot) was computed and the parameters were optimized until a minimum RE value was reached. In our case, this was when p was 4 and j was higher than 100. After a rough approach during which only the quantum yields were optimized, all the parameters were made free in order to refine the final fittings. At the end of the calculation, the set of optimized parameters was proved to be unique.

Acknowledgement

We thank Prof. Gunter Fischer for helpful discussions, Birgit Hökelmann and Bernd Heinrich for technical assistance, Dr. Judith Maria Habazettl and Monika Seidel for NMR analysis, and Mike Thatcher for critical reading of the manuscript.

[1] M. Brandsch, F. Thunecke, G. Kullertz, M. Schutkowski, G. Fischer, K. Neubert, *J. Biol. Chem.* **1998**, *273*, 3861–3864.
[2] I. Willner, *Acc. Chem. Res.* **1997**, *30*, 347–356.
[3] G. Fischer, *Chem. Soc. Rev.* **2000**, *29*, 119–127.
[4] For peptidomimetics or peptide backbone modification, see, for example: a) A. F. Spatola, *Chemistry and Biochemistry of Amino Acids, Peptides and Proteins*, Marcel Dekker, New York, **1983**, pp. 267–357; b) A. Abell, *Advances in Amino Acid Mimetics and Peptidomimetics*, *Vol. 2*, JAI Press, Stamford, **1999**; c) W. Kazmierski, *Peptidomimetic Protocols*, Humana Press, Totowa, **1999**; d) D. Steer, R. Lew, P. Perlmutter, A. Smith, M. Aguilar, *Curr. Med. Chem.* **2002**, *9*, 811–822.
[5] R. Behrendt, C. Renner, M. Schenk, F. Wang, J. Wachtveitl, D. Oesterhelt, L. Moroder, *Angew. Chem.* **1999**, *111*, 2941–2943; *Angew. Chem. Int. Ed.* **1999**, *38*, 2771–2774.
[6] A. Yamazawa, X. Liang, H. Asanuma, M. Komiyama, *Angew. Chem.* **2000**, *112*, 2446–2447; *Angew. Chem. Int. Ed.* **2000**, *39*, 2356–2357.
[7] a) M. Irie, *Chem. Rev.* **2000**, *100*, 1685–1716; b) Y. Yokoyama, *Chem. Rev.* **2000**, *100*, 1717–1739; c) G. Berkovic, V. Krongauz, V. Weiss, *Chem. Rev.* **2000**, *100*, 1741–1753; d) N. Hampp, *Chem. Rev.* **2000**, *100*, 1755–1776; e) S. Kawata, Y. Kawata, *Chem. Rev.* **2000**, *100*, 1777–1788; f) B. L. Feringa, R. A. V. Delden, N. Koumura, E. M. Geertsema, *Chem. Rev.* **2000**, *100*, 1789–1816; g) J. A. Delaire, K. Nakatani, *Chem. Rev.* **2000**, *100*, 1817–1845; h) K. Ichimura, *Chem. Rev.* **2000**, *100*, 1847–1873; i) N. Tamai, H. Miyasaka, *Chem. Rev.* **2000**, *100*, 1875–1890.
[8] a) D. Liu, J. Karanicolas, C. Yu, Z. Zhang, G. A. Woolley, *Bioorg. Med. Chem. Lett.* **1997**, *7*, 2677–2680; b) A. J. Harvey, A. D. Abell, *Bioorg. Med. Chem. Lett.* **2001**, *11*, 2441–2444.
[9] See, for example: a) D. W. Brown, M. M. Campbell, C. V. Walker, *Tetrahedron* **1983**, *39*, 1075–1083; b) K. Clausen, A. F. Spatola, C. Lemieux, P. W. Schiller, S.-O. Lawesson, *Biochem. Biophys. Res. Commun.* **1984**, *120*, 305–310; c) O. E. Jensen, S.-O. Lawesson, R. Bardi, A. M. Piazzesi, C. Toniolo, *Tetrahedron* **1985**, *41*, 5595–5606; d) R. Bardi, A. M. Piazzesi, C. Toniolo, O. E. Jensen, T. P. Andersen, A. Senning, *Tetrahedron* **1988**, *44*, 761–769; e) D. B. Sherman, A. F. Spatola, W. S. Wire, T. F. Burks, T. M. D. Nguyen, P. W. Schiller, *Biochem. Biophys. Res. Commun.* **1989**, *162*, 1126–1132; f) B. D. Sherman, A. F. Spatola, *J. Am. Chem. Soc.* **1990**, *112*, 433–441; g) D. Seebach, S. Y. Ko, H. Kessler, M. Kock, M. Reggelin, P. Schmeider, M. D. Walkinshaw, J. J. Bolsterli, D. Bevec, *Helv. Chim. Acta* **1991**, *74*, 1953–1990; h) H. Kessler, H. Matter, A. Geyer, H.-J. Diehl, M. Koeck, G. Kurz, F. R. Opperdoes, M. Callens, R. K. Wierenga, *Angew. Chem.* **1992**, *104*, 343–345; *Angew. Chem. Int. Ed. Engl.* **1992**, *31*, 328–330; i) H. Kessler, A. Geyer, H. Matter, M. Kock, *Int. J. Pept. Protein Res.* **1992**, *40*, 25–40; j) M. Schutkowski, K. Neubert, G. Fischer, *Eur. J. Biochem.* **1994**, *221*, 455–461; k) R. A. Shaw, E. Kollat, M. Hollosi, H. H. Mantsch, *Spectrochim. Acta A* **1995**, *51*, 1399–1412; l) M. Schutkowski, S. Wöllner, G. Fischer, *Biochemistry* **1995**, *34*, 13016–13026; m) H.-T. Le, R. Michelot, M. Dumont, V. K. Shukla, M. Mayer, K. P.-P. Nguyen, H. Ruan, S. Lemaire, *Can. J. Physiol. Pharmacol.* **1997**, *75*, 9–14; n) J. Lehmann, A. Linden, H. Heimgartner, *Tedrahedron* **1998**, *54*, 8721–8736; o) J. Lehmann, H. Heimgartner, *Helv. Chim. Acta* **1999**, *82*, 1899–1915; p) J. Lehmann, A. Linden, H. Heimgartner, *Tetrahedron* **1999**, *55*, 5359–5376; q) J. H. Miwa, L. Pallivathucal, S. Gowda, K. E. Lee, *Org. Lett.* **2002**, *4*, 4655–4657; r) T. T. Tran, J. Zeng, H. Treutlein, A. W. Burgess, *J. Am. Chem. Soc.* **2002**, *124*, 5222–5230; s) J. Helbing, H. Bregy, J. Bredenbeck, R. Pfister, P. Hamm, R. Huber, J. Wachtveitl, L. D. Vico, M. Olivucci, *J. Am. Chem. Soc.* **2004**, *126*, 8823–8834.
[10] R. Frank, M. Jakob, F. Thunecke, G. Fischer, M. Schutkowski, *Angew. Chem.* **2000**, *112*, 1163–1165; *Angew. Chem. Int. Ed.* **2000**, *39*, 1120–1122.
[11] Y. Hitotsuyanaagi, S. Motegi, H. Fukaya, K. Takeya, *J. Org. Chem.* **2002**, *67*, 3266–3271.
[12] S. A. Hart, F. A. Etzkorn, *J. Org. Chem.* **1999**, *64*, 2998–2999.
[13] U. Reimer, N. E. Mokdad, M. Schutkowski, G. Fischer, *Biochemistry* **1997**, *36*, 13802–13808.
[14] J. Holtz, P. Li, S. A. Asher, *J. Am. Chem. Soc.* **1999**, *121*, 3762–3766.
[15] G. Fischer, *Angew. Chem.* **1994**, *106*, 1479–1501; *Angew. Chem. Int. Ed. Engl.* **1994**, *33*, 1415–1436.
[16] G. Scherer, M. K. Kramer, M. Schutkowski, U. Reimer, G. Fischer, *J. Am. Chem. Soc.* **1998**, *120*, 5568–5574.
[17] C. Schiene-Fischer, G. Fischer, *J. Am. Chem. Soc.* **2001**, *123*, 6227–6231.

[18] *Circular Dichroism: Principles and Applications* (Eds.: K. Nakanishi, N. Berova, R. W. Woody), VCH, New York, **1994**.
[19] G. Pappenberger, H. Aygun, J. W. Engels, U. Reimer, G. Fischer, T. Kiefhaber, *Nat. Struct. Biol.* **2001**, *8*, 452–458.
[20] I. Harada, M. Tasumi, *Chem. Phys. Lett.* **1980**, *70*, 279–282.
[21] C. Kato, H. Hamaguchi, M. Tasumi, *J. Phys. Chem.* **1985**, *89*, 407–410.
[22] T. Sifferlen, M. Rueping, K. Gademann, B. Jaun, D. Seebach, *Helv. Chim. Acta* **1999**, *82*, 2067–2093.
[23] J. Zhao, D. Wildemann, M. Jakob, C. Vargas, C. Schiene-Fischer, *Chem. Commun.* **2003**, 2810–2811.
[24] S. Meyer, A. Jabs, M. Schutkowski, G. Fischer, *Electrophoresis* **1994**, *15*, 1151–1157.
[25] J. Blanc, D. L. Ross, *J. Phys. Chem.* **1968**, *72*, 2817–2824.
[26] D. Lauvergnat, P. C. Hiberty, *J. Am. Chem. Soc.* **1997**, *119*, 9478–9482.
[27] For the protected peptide **4**, however, the isomerization rate constant was independent of the pH value because its N and C termini were protected (the k_{obsd}/pH profile is a horizontal line; data not shown). For this kind of protected peptide, it is impossible to study the isomerization with the pH-jump method. Instead, it is very convenient to perform the same study with the photoswitch method.
[28] N. J. Baxter, M. P. Williamson, *J. Biomol. NMR* **1997**, *9*, 359–369.
[29] D. Kern, M. Schutkowski, T. Drakenberg, G. Fischer, *J. Am. Chem. Soc.* **1997**, *119*, 8403–8408.
[30] *Photochromism, Molecules and Systems* (Eds.: H. Durr, H. Bouas-Laurent), Elsevier, New York, **1990**.
[31] M. H. Deniel, D. Lavabre, J. C. Micheau in *Organic Photochromic and Thermochromic Compounds, Vol. 2* (Eds.: J. C. Crano, R. J. Guglielmetti), Plenum Publishers, New York, **1999**, pp. 167–210.
[32] H. Rau, G. Greiner, *J. Phys. Chem.* **1990**, *94*, 6523–6524.
[33] G. Favaro, V. Malatesta, U. Mazzucato, G. Ottavi, A. Romani, *J. Photochem. Photobiol. A* **1995**, *87*, 235–241.
[34] V. Pimienta, D. Lavabre, G. Levy, A. Samat, R. Guglielmetti, J. C. Micheau, *J. Phys. Chem.* **1996**, *100*, 4485–4490.
[35] P. Li, X. Chen, E. Shulin, S. Asher, *J. Am. Chem. Soc.* **1997**, *119*, 1116–1120.
[36] E. Fischer, *J. Phys. Chem.* **1967**, *71*, 3704–3705.
[37] O. Pieroni, A. Fissi, F. Ciardelli, D. Fabbri, *Mol. Cryst. Liq. Cryst.* **1984**, *246*, 191–194.
[38] D. James, D. Burns, G. Woolley, *Protein Eng.* **2001**, *14*, 983–991.
[39] D. Wildemann, M. Drewello, G. Fischer, M. Schutkowski, *Chem. Commun.* **1999**, 1809–1810.

Received: April 23, 2004
Revised: August 2, 2004
Published online: October 29, 2004

